ACADEMIC PRESS

Available online at www.sciencedirect.com
SCIENCE DIRECT®

Journal of Solid State Chemistry 171 (2003) 339–344

JOURNAL OF SOLID STATE CHEMISTRY

http://elsevier.com/locate/jssc

Al substitution effects to the magnetic properties of the compounds in the Sm–Fe system

H. Samata,[a,*] R. Kasai,[b] T. Taniguchi,[b] and Y. Nagata[b]

[a] *Faculty of Mercantile Marine Science, Kobe University of Mercantile Marine, Fukaeminami, Higashinada, Kobe 658-0022, Japan*
[b] *College of Science and Engineering, Aoyama Gakuin University, Chitosedai, Setagaya, Tokyo 157-8572, Japan*

Received 16 April 2002; received in revised form 25 August 2002; accepted 28 August 2002

Abstract

$Sm(Fe_{1-x}Al_x)_2$, $Sm(Fe_{1-x}Al_x)_3$, $Sm_6(Fe_{1-x}Al_x)_{23}$, and $Sm(Fe_{1-x}Al_x)_7$ crystals were grown by a modified self-flux method, and their magnetic properties were investigated. The saturation magnetization of all compounds decreases by Al substitution. With the Al substitution, the anisotropy field decreases in the $Sm(Fe_{1-x}Al_x)_3$ and $Sm(Fe_{1-x}Al_x)_7$ systems, while in cubic $Sm(Fe_{1-x}Al_x)_2$ and $Sm_6(Fe_{1-x}Al_x)_{23}$ systems it increases considerably. The Curie temperatures of the compounds are dependent on the average distance between the nearest neighbor Fe atoms.

Keywords: Sm–Fe system; $Sm(Fe_{1-x}Al_x)_2$; $Sm(Fe_{1-x}Al_x)_3$; $Sm_6(Fe_{1-x}Al_x)_{23}$; $Sm(Fe_{1-x}Al_x)_7$; Single crystal; Magnetic properties

1. Introduction

Intermetallic compounds in the systems of rare-earth and transition metal have excellent practical magnetic properties and have been widely utilized as permanent magnets, magnetostrictive materials, and magnetic recording media. Among these systems, the Sm–Fe system has been the focus of considerable attention and extensive studies because a notable improvement in hard magnetic properties was attained by the nitrogenation of Sm_2Fe_{17} [1,2]. In addition to Sm_2Fe_{17}, the compounds $SmFe_2$, $SmFe_3$, Sm_6Fe_{23}, and $SmFe_7$ have been reported to exist in the Sm–Fe system [3–10]. Although it is well-known that these compounds show interesting magnetic properties, further improvement in magnetic properties is strongly required for practical use. It is well accepted that the hard magnetic properties of intermetallic compounds of rare-earth and transition metal are improved by the substitution of non-magnetic elements, such as B, Al, and N. The effects of Al substitution on the magnetic properties of $SmFe_7$ were recently investigated using single crystalline specimens [11]. The Curie temperature T_C of $SmFe_7$ increases with a small Al substitution in spite of there being little change in the saturation magnetization M_s. However, it was revealed that Al substitution is ineffective in changing the direction of the easy axis of magnetization. Except for studies on the effects of Al substitution on Sm_2Fe_{17} [12,13] and $SmFe_7$, there has been no systematic study about the effects of the substitution on the magnetic properties of other compounds such as, $SmFe_2$, $SmFe_3$, and Sm_6Fe_{23}. This seems to be due to the difficulties in the crystal growth of these compounds. Recently, a new technique was developed for the crystal growth of the compounds in the Sm–Fe system by modifying the self-flux method [14]. In this study, the effects of Al substitution were studied systematically on $Sm(Fe_{1-x}Al_x)_2$, $Sm(Fe_{1-x}Al_x)_3$, and $Sm_6(Fe_{1-x}Al_x)_{23}$ crystals grown by the new technique.

2. Experimental

Single crystals were grown by a modified self-flux method using excess Sm as a flux [14]. The starting mixture was prepared by arc-melting in a zirconium-gettered argon atmosphere using high-purity Sm (99.9 wt%), Fe (99.9 wt%), and Al (99.9 wt%). The Sm:(Fe + Al) composition ratios of the starting mixture were 55:45–60:40. The starting mixture was placed in an

*Corresponding author. Fax: +81-78-431-6285.
E-mail address: samata@cc.kshosen.ac.jp (H. Samata).

0022-4596/03/$ - see front matter © 2003 Elsevier Science (USA). All rights reserved.
doi:10.1016/S0022-4596(02)00230-X

alumina crucible that had been coated with boron nitride. The alumina crucible was further sealed in a quartz ampoule with argon gas at 460 Torr after being evacuated to 5×10^{-5} Torr. Zirconium shot was used as an oxygen getter to prevent the oxidation of the mixture. The ampoule was heated above the dissolution temperature of the mixture (920–1000°C) in an electric furnace. After being held at that temperature for 0.5–6 h, the ampoule was cooled to 750–800°C at a rate of 0.4–1°C/h. The mixture was then cooled to room temperature by turning off the electric furnace after the slow cooling process had been completed. Exposing the crucible to the ambient atmosphere causes the Sm-flux to change into oxide powder within a few days, which allows the crystals to be removed easily from the bottom of the crucible without applying any mechanical strain. The composition ratio of the starting mixture, cooling temperature range, and cooling rate were changed for each compounds. [7,9,15,16]

The chemical composition of the various crystals was determined by electron-probe microanalysis (EPMA) using wavelength dispersive spectrometers. The crystal structure was characterized by X-ray powder diffraction using Cu$K\alpha$ radiation, and the diffraction data was refined by the Rietveld method [17]. The crystallographic directions of the crystals were determined by the X-ray Laue back-reflection method. Magnetization measurements were performed using a vibrating sample magnetometer (VSM) and a SQUID magnetometer at temperatures from 20 to 800 K in applied magnetic fields up to 20 kOe and at temperatures from 5 to 350 K in applied magnetic fields up to 50 kOe, respectively. In order to prevent the oxidation of the specimens, high-temperature (300–800 K) magnetization measurements were performed on specimens that had been sealed in a quartz sample tube after evacuation to 3×10^{-5} Torr.

3. Results and discussion

3.1. Crystallographic and magnetic properties of $Sm(Fe_{1-x}Al_x)_2$

Octahedral crystals were grown on the surface of the flux that remained at the bottom of the crucible. The crystals had natural surfaces with metallic luster and were $1.0 \times 1.0 \times 1.0$ mm in size at the maximum. The results of microanalysis indicated that the crystal had the chemical composition of $Sm(Fe_{0.89}Al_{0.11})_2$. The X-ray powder diffraction data could be fitted by assuming a cubic $MgCu_2$-type structure of space group $Fd3m$ and a lattice constant of $a = 0.7472$ nm. This value was slightly larger than that of $SmFe_2$ (0.7425 nm) [15]. Since the metallic bond radius of Al (0.143 nm) is larger than that of Fe (0.124 nm), the lattice constant must be expanded by the Al substitution.

Fig. 1 shows the temperature dependence of the magnetization measured under an applied magnetic field of 50 Oe. The inset of the figure shows the temperature derivative of the magnetization. The derivative dM/dT shows that the Curie temperature T_C of $Sm(Fe_{0.89}Al_{0.11})_2$ is 600 K. This value is lower than that of $SmFe_2$ (670 K). It is well known that the T_C of rare-earth and iron compounds depends on the exchange interaction between Fe–Fe atoms. The Al substitution will reduce the number of Fe–Fe interactions and then decrease the T_C. Fig. 2a shows the magnetic-field dependence of magnetization measured at 5 K by applying a magnetic field parallel to the [110], [111], and [100] directions of the cubic crystal. The magnetization tends to be saturated in the [110] direction, while, in the [100] direction, it could not be saturated up to 50 kOe. These results indicate that the easy and hard directions of magnetization are parallel to the [110] and [100] directions, respectively. Magnetization curves measured at 300 K are shown in Fig. 2b. The easy and hard directions of magnetization are parallel to the [111] and [100] directions, respectively. These results indicate that the easy direction changes at a temperature between 5 and 300 K. The saturation magnetization M_s at 5 and 300 K are 60.8 emu/g and 55.0 emu/g, respectively. These values are lower than those of $SmFe_2$ (64.4 emu/g at 5 K and 59.8 emu/g at 300 K). This would be due to the magnetic dilution caused by the substitution of non-magnetic Al. In general, the cubic magnetocrystalline anisotropy constants K_1 and K_2 can be estimated roughly from the area enclosed by the magnetization curves [18]. $K_1 = -1.0 \times 10^7$ erg/cm^3 and $K_2 = -2.3 \times 10^7$ erg/cm^3 were deduced from the magnetization data at 300 K. Fig. 3 shows the temperature dependence of magnetizations measured in the

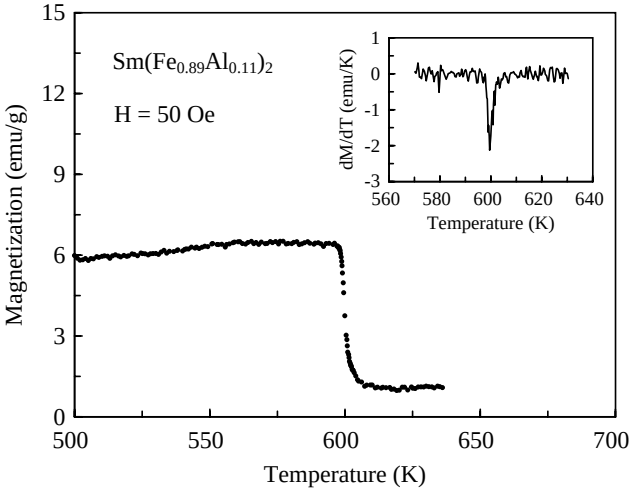

Fig. 1. Temperature dependence of the magnetization measured for a $Sm(Fe_{0.89}Al_{0.11})_2$ crystal under applied magnetic fields of 50 Oe. The inset shows the temperature dependence of the temperature derivative of the magnetization.

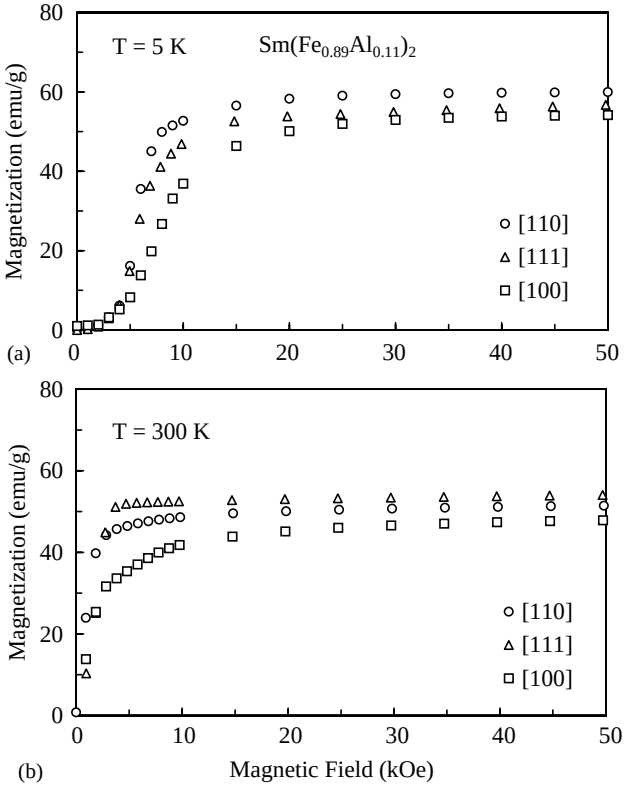

Fig. 2. Field dependence of magnetization measured for a $Sm(Fe_{0.89}Al_{0.11})_2$ crystal at 5 K (a) and 300 K (b) in the [110], [111], and [100] directions of the cubic crystal.

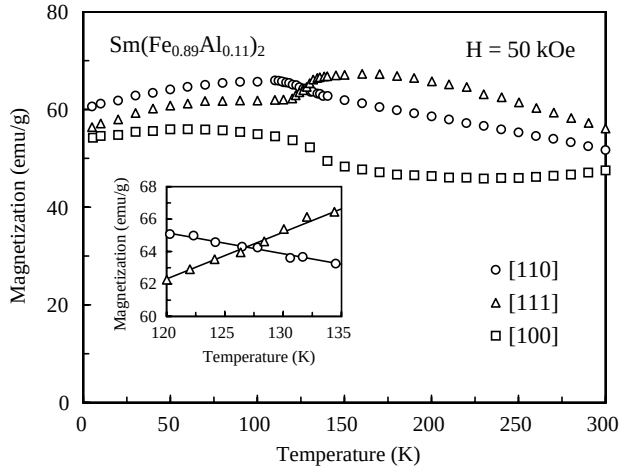

Fig. 3. Temperature dependence of magnetizations measured for a $Sm(Fe_{0.89}Al_{0.11})_2$ crystal in the [110], [111], and [100] directions under an applied field of 50 kOe. The inset shows the enlarged view near the crossover point.

[110], [111], and [100] directions under an applied magnetic field of 50 kOe. The direction in which the largest magnetization is observed changes from the [110] direction to the [111] direction at 127 K, indicating that a crossover of the easy direction of magnetization takes place at this temperature. This crossover temperature of $Sm(Fe_{0.89}Al_{0.11})_2$ is much smaller than that of $SmFe_2$ (195 K), which suggests that iron makes a great contribution to the magnetic anisotropy of $SmFe_2$.

3.2. Crystallographic and magnetic properties of $Sm(Fe_{1-x}Al_x)_3$

$Sm(Fe_{1-x}Al_x)_3$ crystals had a distinct natural surface with a large hexagonal plane and a maximum size of $3.0 \times 3.0 \times 1.0$ mm. The X-ray powder diffraction data could be fitted by assuming a rhombohedral $PuNi_3$-type structure of the space group of $R3m$ and lattice constants of $a = 0.5198$ nm and $c = 2.4877$ nm in the hexagonal description. Those values were slightly larger than those of $SmFe_3$ ($a = 0.5179$ nm and $c = 2.4795$ nm) [7]. As in the case of $Sm(Fe_{1-x}Al_x)_2$, the crystal lattice was expanded by the Al substitution. The large hexagonal plane of the as-grown crystal was confirmed to be the c-plane of the hexagonal crystal by the X-ray Laue back-reflection method.

The temperature dependence of the magnetization measured in a low field of 5 Oe is shown in Fig. 4. The Curie temperature of the $Sm(Fe_{0.90}Al_{0.10})_3$ crystal is determined to be 590 K from the temperature dependence of dM/dT. This value is much lower than that of $SmFe_3$ (640 K). A considerable amount of magnetization can be observed above the T_C. This is due to the precipitation of αFe, which is caused by the decomposition of $Sm(Fe_{0.90}Al_{0.10})_3$. Fig. 5 shows the temperature dependence of the magnetization measured in the field of 10 kOe applied parallel to the c-axis. The magnetization increases as the temperature decreases but tends to decrease below 120 K due to a change in the easy direction of magnetization. In the $SmFe_3$ crystal, the

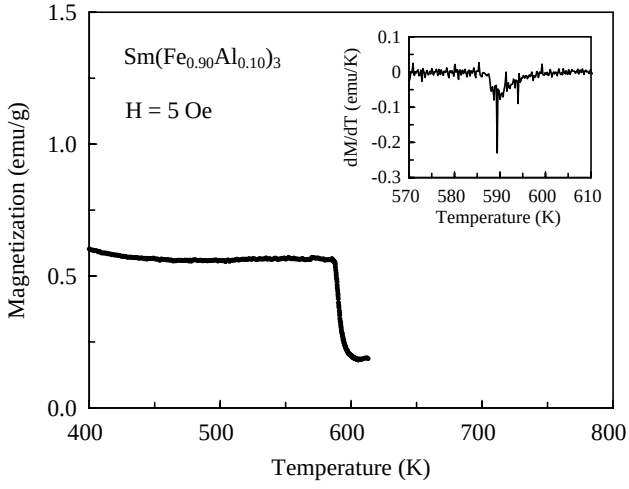

Fig. 4. Temperature dependence of the magnetization measured for a $Sm(Fe_{0.90}Al_{0.10})_3$ crystal in an applied field of 5 Oe. The inset shows the temperature dependence of the temperature derivative of the magnetization.

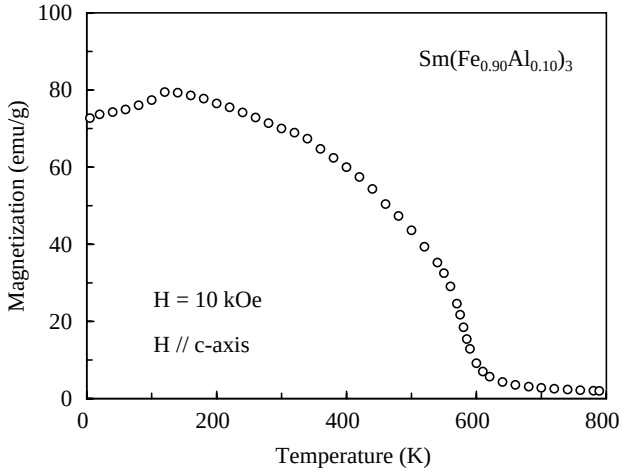

Fig. 5. Temperature dependence of the magnetization measured for a $Sm(Fe_{0.90}Al_{0.10})_3$ crystal in the field of 10 kOe applied parallel to the *c*-axis.

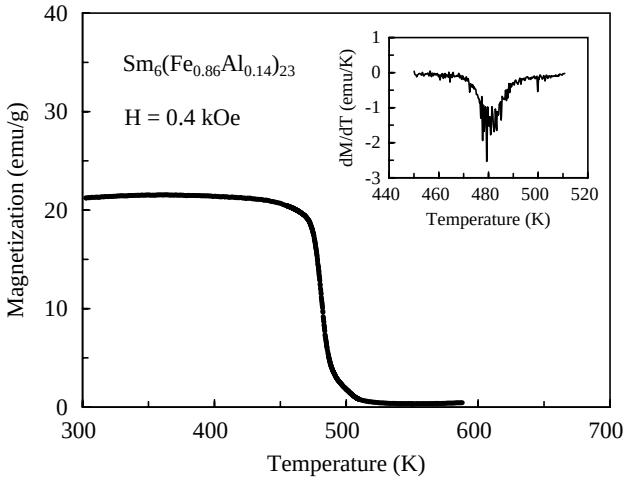

Fig. 6. Temperature dependence of the magnetization measured for a $Sm_6(Fe_{0.86}Al_{0.14})_{23}$ crystal in the magnetic field of 0.4 kOe. The inset shows the temperature dependence of the temperature derivative of the magnetization.

easy direction is parallel to the *c*-axis at 300 K, however, it lies on the surface of a cone at temperatures below 160 K [7]. In order to confirm the phenomenon precisely, the magnetic anisotropy of the $Sm(Fe_{0.90}Al_{0.10})_3$ crystal was characterized by the relation $H/M = 2K_1/M_s^2 + 4K_2M^2/M_s^4$ using the data of magnetization measurements [7]. The anisotropy constants, which are determined by magnetization measurements at 5 and 300 K, are $K_1 = -2.3 \times 10^6$ and $K_2 = 2.7 \times 10^6$ erg/cm^3 and $K_1 = 1.7 \times 10^7$ and $K_2 = 1.5 \times 10^7$ erg/cm^3, respectively. In the hexagonal system, the easy direction of magnetization lies on the surface of a cone when $K_1 < 0$ and $K_1 + 2K_2 > 0$ [19], and the half-cone angle θ is given by the relation $\theta = \sin^{-1}(-K_1/2K_2)^{1/2}$. $\theta = 40^\circ$ was deduced at 5 K using the values of K_1 and K_2. This value is larger than that of $SmFe_3$ ($\theta = 31^\circ$). In the $Sm(Fe_{0.90}Al_{0.10})_3$, the tilt of the easy direction of magnetization occurs at 120 K, which is lower than that of $SmFe_3$ (160 K). The peculiar thermomagnetic curve observed in Fig. 5 is easily explained by the tilt of the easy direction.

3.3. Magnetic properties of $Sm_6(Fe_{1-x}Al_x)_{23}$

Nearly cubic crystals with a natural habit and metallic luster grew on the bottom of the crucible. The maximum size of the crystals was about $1.0 \times 1.0 \times 1.0$ mm. The result of EPMA indicated that the crystals had the chemical composition of $Sm_6(Fe_{0.86}Al_{0.14})_{23}$. It was confirmed by the X-ray Laue back-reflection method that the natural surfaces of the crystal were the {111} and {100} planes of the cubic crystal. Fig. 6 shows the temperature dependence of the magnetization measured in magnetic fields of 0.4 kOe. The Curie temperature of $Sm_6(Fe_{0.86}Al_{0.14})_{23}$ was determined to be 480 K from the temperature dependence of dM/dT. In spite of the Al substitution, the T_C of $Sm_6(Fe_{0.86}Al_{0.14})_{23}$ is higher than that of Sm_6Fe_{23} (442 K). This is different from the cases

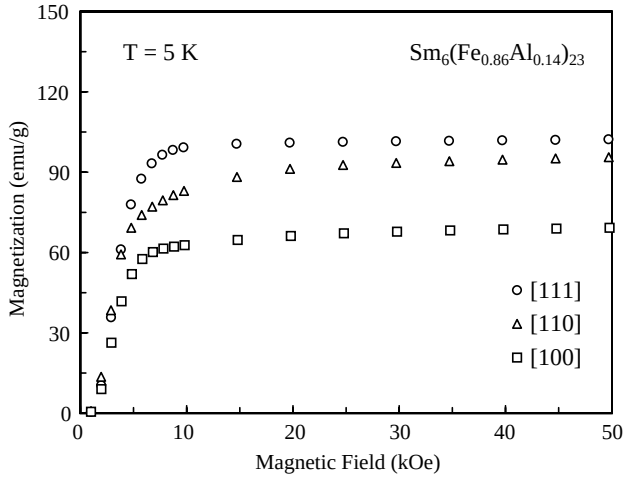

Fig. 7. Field dependence of magnetization measured for a $Sm_6(Fe_{0.86}Al_{0.14})_{23}$ crystal at 5 K in the [111], [110], and [100] directions of the cubic crystal.

of $Sm(Fe_{1-x}Al_x)_2$ and $Sm(Fe_{1-x}Al_x)_3$. In the $Sm_6(Fe_{1-x}Al_x)_{23}$ system, Al substitution seems effective to increase the Curie temperature. The magnetization curves measured along the three principal crystallographic directions of cubic crystal at 5 K are shown in Fig. 7. The magnetization along the [111] direction tends to be saturated above 10 kOe, while that along the [100] direction does not saturate up to 50 kOe and seems to require a fairly large magnetic field to saturate the magnetization. In the $Sm_6(Fe_{1-x}Al_x)_{23}$ system, no change of the easy and hard directions of magnetization was observed between 5 and 300 K. The saturation magnetization M_s at 5 and 300 K are 103 and 58.3 emu/g, respectively. These values are smaller than those of Sm_6Fe_{23} (151 emu/g at 300 K and 64.4 emu/g at 5 K) [16]. As in the case of other Sm–Fe compounds,

Table 1
Effects of Al substitution on the basic magnetic properties

	$Sm(Fe_{1-x}Al_x)_2$ cubic		$Sm(Fe_{1-x}Al_x)_3$ rhombohedral		$Sm_6(Fe_{1-x}Al_x)_{23}$ cubic		$Sm(Fe_{1-x}Al_x)_7$ [11,20] tetragonal	
	$x=0$	$x=0.11$	$x=0$	$x=0.10$	$x=0$	$x=0.14$	$x=0$	$x=0.12$
M_s (emu/g)	59.8	55.0	80.7	70.0	64.4	58.3	136	83.5
T_C (K)	670	600	640	590	442	480	602	515
K_1 (erg/cm^3)	-5.1×10^6	-1.0×10^7	2.4×10^7	1.7×10^7	-2.7×10^6	-7.4×10^6	-8.7×10^7	-9.7×10^7
K_2 (erg/cm^3)	1.7×10^6	-2.3×10^7	2.2×10^7	1.5×10^7	6.3×10^5	3.8×10^6	1.4×10^7	3.8×10^7
H_A (kOe)	12	51	72	61	6	19	110	70

saturation magnetization is decreased by the dilution of the Fe sublattice. On the other hand, the anisotropy constants of $K_1=-7.4\times10^6$ and $K_2=3.8\times10^6$ erg/cm^3 are deduced from the magnetization curves at 300 K. This result suggests that Al substitution is effective in increasing the anisotropy constants.

3.4. Effects of Al substitution on Sm–Fe compounds

Table 1 shows the effects of Al substitution on the basic magnetic properties of Sm–Fe compounds at 300 K except for T_C. The anisotropy fields H_A of $Sm(Fe_{1-x}Al_x)_2$ and $Sm_6(Fe_{1-x}Al_x)_{23}$ were calculated using the relation of $H_A=-(4/3)\{K_1+(K_2/3)\}/M_s$, while those of hexagonal $Sm(Fe_{1-x}Al_x)_3$ and tetragonal $Sm(Fe_{1-x}Al_x)_7$ were deduced by the relations of $H_A=2K_1/M_s$ and $H_A=-2(K_1+2K_2)/M_s$, respectively. The M_s of all compounds decreases with Al substitution. This is thought to be due to the magnetic dilution in the Fe sublattice. In the $Sm(Fe_{1-x}Al_x)_3$ and $Sm(Fe_{1-x}Al_x)_7$ systems, H_A decreases with the substitution of Al, while, in a cubic structure such as $Sm(Fe_{1-x}Al_x)_2$ and $Sm_6(Fe_{1-x}Al_x)_{23}$, H_A increases significantly with Al substitution. In general, the spin moment of rare-earth ions couples strongly with the orbital angular momentum, and the magnetocrystalline anisotropy of rare-earth compounds is thus strongly influenced by the geometric configuration of the 4*f*-orbital of rare-earth ions at low temperature. The configuration of the 4*f*-orbital is determined by the geometric configuration of ligand rare-earth ions. Therefore, when the Al substitution increases the lattice constants *c* of $Sm(Fe_{1-x}Al_x)_3$ and $Sm(Fe_{1-x}Al_x)_7$ systems, the freedom in the geometric configuration of the 4*f*-obital of Sm^{3+} is increased, and then the magnetocrystalline anisotropy is decreased. On the other hand, in the cubic $Sm(Fe_{1-x}Al_x)_2$ and $Sm_6(Fe_{1-x}Al_x)_{23}$ systems, the configuration of the 4*f*-obital of Sm^{3+} seems to become more stable in the [111] direction as a result of Al substitution.

Fig. 8 shows the T_C of the $Sm(Fe_{1-x}Al_x)_2$, $Sm(Fe_{1-x}Al_x)_3$, $Sm_6(Fe_{1-x}Al_x)_{23}$, and $Sm(Fe_{1-x}Al_x)_7$ systems as a function of the average distance between the nearest neighbor Fe atoms. The Curie temperature increases as the Fe atomic distance increases between

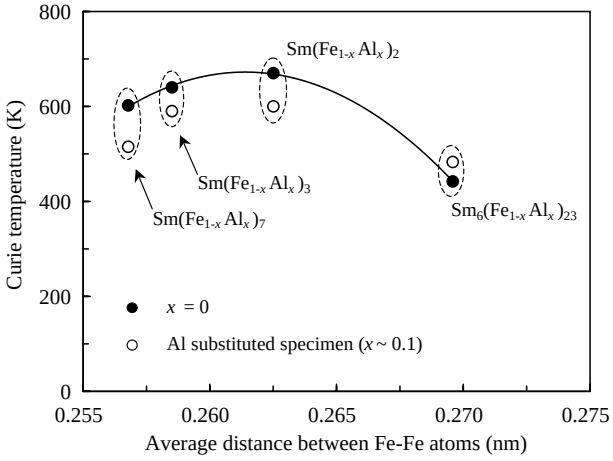

Fig. 8. Curie temperature determined for various Sm–Fe compounds as a function of the average nearest Fe–Fe distance.

0.256 and 0.262 nm (from $SmFe_7$ to $SmFe_2$) but tends to decrease over 0.262 nm. Moreover, in the $Sm(Fe_{1-x}Al_x)_7$ system, the T_C is increased by the substitution of a small amount of Al ($x\leqslant0.07$) [11]. However, the T_C decreases when the Al substitution increases over $x=0.10$. It is well accepted that the T_C of rare-earth and transition metal compounds is determined by the exchange interaction between TM atoms. The increase in T_C can be explained by the expansion of the nearest neighbor Fe atomic distance, which is caused by substituting a small amount of Al. However, the T_C will decrease when the number of Fe–Fe pairs is decreased by further Al substitution. The reduction of T_C observed in the $Sm(Fe_{1-x}Al_x)_3$ and $Sm(Fe_{1-x}Al_x)_2$ systems can also be explained by the reduction of the number of Fe–Fe pairs. However, the reason for the enhancement of T_C in the $Sm_6(Fe_{1-x}Al_x)_{23}$ system is unclear at present, it is necessary to investigate the preferred occupation of sites by the Al atoms on the crystals with various Al compositions.

4. Conclusion

$Sm(Fe_{1-x}Al_x)_2$, $Sm(Fe_{1-x}Al_x)_3$, $Sm_6(Fe_{1-x}Al_x)_{23}$, and $Sm(Fe_{1-x}Al_x)_7$ crystals were grown by a modified

self-flux method, and their magnetic properties were investigated. The saturation magnetization of all compounds is decreased by the non-magnetic Al substitution. In the $Sm(Fe_{1-x}Al_x)_3$ and $Sm(Fe_{1-x}Al_x)_7$ systems, the anisotropy field is decreased with the Al substitution, while, in the cubic $Sm(Fe_{1-x}Al_x)_2$ and $Sm_6(Fe_{1-x}Al_x)_{23}$ systems, it is increased significantly. The Curie temperature of these compounds seems to be dependent on the average distance between the nearest neighbor Fe atoms.

Acknowledgments

The work performed at Aoyama Gakuin University was supported by a Grant-in-Aid for Scientific Research from the Ministry of Education, Science, Sports and Culture, Japan.

References

[1] J.M.D. Coey, Hong Sun, J. Magn. Magn. Mater. 87 (1990) 251–254.
[2] T. Iriyama, K. Kobayashi, N. Imaoka, T. Fukuda, H. Kato, Y. Nakagawa, IEEE Trans. Magn. 28 (1992) 2326–2331.
[3] A.E. Clark, Ferromagnetic Materials North-Holland, Amsterdam, Vol. 1, 1980, p. 531.
[4] M. Rosen, H. Klimker, U. Atzmony, M.P. Dariel, Phys. Rev. B 9 (1974) 254–258.
[5] K.H.J. Buschow, J. Less-Common Met. 25 (1971) 131–134.
[6] J. Wecker, M. Katter, K. Schnitzke, L. Schultz, J. Appl. Phys. 69 (1991) 5847–5849.
[7] H. Samata, N. Fujiwara, Y. Shimizu, Y. Nagata, T. Uchida, M.D. Lan, Jpn. J. Appl. Phys. 36 (1997) 3492–3496.
[8] W. Zarek, M. Pardavi-Horvath, Z. Obuszko, J. Magn. Magn. Mater. 21 (1980) 47–50.
[9] H. Samata, Y. Satoh, Y. Nagata, T. Uchida, M. Kai, M.D. Lan, Jpn. J. Appl. Phys. 36 (1997) 476–478.
[10] K.H.J. Buschow, J. Less-Common Met. 11 (1966) 204–208.
[11] H. Samata, M. Kamonji, H. Sasaki, S. Yashiro, M. Kai, T. Uchida, Y. Nagata, J. Alloy. Compd. 311 (2000) 130–136.
[12] H. Kato, J. Shiomi, T. Koide, T. Iriyama, M. Yamada, Y. Nakagawa, J. Alloy. Compd. 222 (1995) 62–66.
[13] Yang Fu-ming, Li Xin-wen, N. Tang, Wang Jian-li, Lu Zhonghua, Zhao Tong-yun, Li Qing-an, F.R. de Boer, J.P. Liu, J. Alloy. Compd. 221 (1995) 248–253.
[14] H. Samata, K. Sakamoto, S. Yashiro, Y. Nagata, J. Cryst. Growth 229 (2001) 482–486.
[15] H. Samata, N. Fujiwara, Y. Nagata, T. Uchida, M.D. Lan, Jpn. J. Appl. Phys. 37 (1998) 5544–5548.
[16] H. Samata, T. Uchida, Y. Shimizu, S. Sato, S. Yashiro, Y. Nagata, J. Alloy. Compd. 322 (2001) 37–41.
[17] F. Izumi, T. Ikeda, Mater. Sci. Forum 321–324 (2000) 198–203.
[18] G.M. Kalvius, R.S. Tebble (Eds.), Experimental Magnetism, Wiley, New York, 1979, p. 188.
[19] K. Ohta, Jiki Kogaku no Kiso II, Kyoritsu Shuppan, Tokyo, 1973, p. 224.
[20] H. Samata, N. Fujiwara, Y. Nagata, T. Uchida, M.D. Lan, Jpn. J. Appl. Phys. 37 (1998) 3290–3294.